Control of Dual Three-Phase Permanent Magnet Synchronous Machine Based on Five-Leg Inverter

Yashan Hu, Shoudao Huang, *Senior Member, IEEE*, Xuan Wu, and Xuefei Li

***Abstract*—This paper proposes a current control of dual three-phase permanent magnet synchronous machine (PMSM) based on five-leg inverter. The five-leg inverter can be utilized to drive dual three-phase PMSM with full torque at slow speed when the conventional dual three-phase voltage source inverter (VSI) has a faulty inverter leg. Usually, the common leg in the five-leg inverter may have severe current stress. By dedicated selection of which two phases as a pair to share the common leg, its current rating is approximately half of current rating of other legs. Meanwhile, the five-leg inverter can fully fulfill the vector space decomposition control for dual three-phase PMSM, which has the same dynamical performance as the conventional dual three-phase VSI. However, due to the asymmetry of five-leg inverter non-linearity, the currents of dual three-phase PMSM are unbalanced. To mitigate this issue, the five-leg inverter non-linearity compensation is also introduced and investigated in this paper, whose effectiveness is verified by comparative experiments on a prototype dual three-phase PMSM.**

***Index Terms*—Double star machine, dual three-phase permanent magnet synchronous machine (PMSM), five-leg inverter, six-phase machine.**

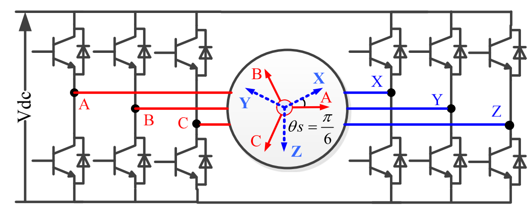

Fig. 1. Conventional dual three-phase VSI [8].

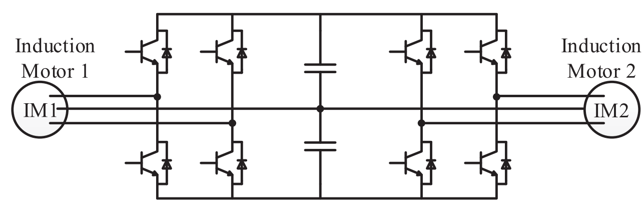

Fig. 2. Four-leg inverter topology [11], [12].

I. Introduction

DUAL three-phase machine is an attractive candidate in industry due to its high reliability [1]–[6], reduced torque pulsation [7], and high efficiency [3]. The dual three-phase machine fed by conventional dual three-phase voltage source inverters (VSIs) is shown in Fig. 1 [8]. It is constructed by two sets of single three-phase VSIs, which share the common dc bus. The dual three-phase machine consists of two sets of single three-phase windings, one set being designated as *ABC*, and the other set as *XYZ* shifted by 30° electrical degrees.

When the conventional dual three-phase inverter has a faulty inverter leg, it must operate in reduced-switch converter operation. The reduced-switch inverter has been extensively studied in single three-phase drive system previously. For example, the midpoint of dc bus capacitors or midpoint of two independent dc voltage sources are assisted to drive one of the three-phase windings; therefore, only four power switches (two inverter legs) are required and the inverter is named as B4 inverter [9], [10].

Considering the reduced-switch converter operation for dual three-phase system, a four-leg inverter with the access of midpoint of dc bus capacitors shown in Fig. 2 can be utilized. For example, the rectifier and inverter in a single three-phase rectifier/inverter back-to-back system share the same midpoint of dc bus capacitors in [11]. The four-leg inverter is employed to drive two independent induction machines, which can be controlled individually in [12]. Therefore, the four-leg inverter is also applicable to drive the dual three-phase machine. However, there are large dc bus voltage fluctuation and circulating currents through the dc bus capacitors [11], [12]. Therefore, bulky, costly, and reliable capacitors are required in practice.

Another attractive reduced-switch operation for dual three-phase system is the five-leg inverter operation. There are two kinds of topologies that are applicable for dual three-phase machine.

The first topology 1 is shown in Fig. 3(a), where one phase of the first three-phase system (M1) is connected to the neutral point of the second three-phase system (M2) [13], [14]; therefore, the zero sequence current of M2 will be the phase current of M1. Since the zero-sequence current does not contribute to torque, there are no zero sequence components in the back electromotive force (EMF). The topology 1 has the capability of fully independent control of two individual machines

Manuscript received July 11, 2018; revised September 21, 2018 and January 4, 2019; accepted February 5, 2019. Date of publication February 18, 2019; date of current version August 29, 2019. This work was supported by the Fundamental Research Funds for the Central Universities under Grant 531107051187. Recommended for publication by Associate Editor Y. A.-R. I. Mohamed. *(Corresponding author: Yashan Hu.)*

The authors are with the College of Electrical and Information Engineering, Hunan University, Changsha 410082, China (e-mail:

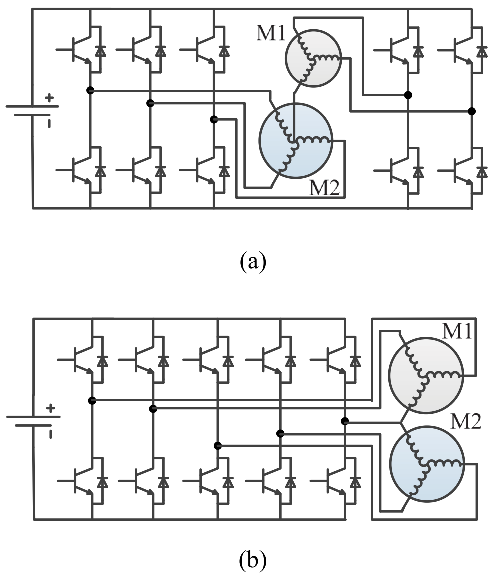

Fig. 3. Five-leg inverter. (a) Topology 1 [16]. (b) Topology 2 [13].

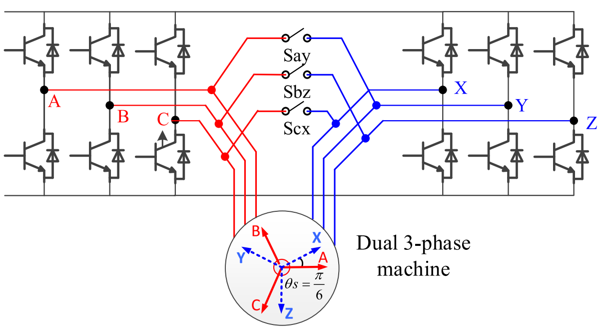

Fig. 4. Fault-tolerant control of dual three-phase machine.

[13]–[15]. However, it is only applicable when the current rating of M1 is much smaller than that of M2, so this topology is not suitable to the dual three-phase permanent magnet synchronous machine (PMSM) as the current rating of each single three-phase winding is the same.

The second topology 2 is shown in Fig. 3(b), where the common leg is shared by one phase in each individual single three-phase system [16]–[20]. As the three-phase currents depend on the line voltages without access of the neutral point, the currents of the two single three-phase systems can be controlled independently. However, the current of the common leg is the sum current of the two phases sharing the common leg; consequently, it may have severe current stress issue of overload.

The five-leg inverter can be applied in the application of fault-tolerant control of dual three-phase machine. The conventional dual three-phase inverter in Fig. 1 can be re-configured as a five-leg inverter manually or automatically when it has one faulty inverter leg. One potential reconfiguration is illustrated in Fig. 4, e.g., if inverter leg-X is faulty and isolated from the system, the switch Scx is switched ON, then phases *X* and *C* will share the common leg *C*. Compared with the conventional fault tolerant control with only phase windings *ABC* working, which can provide only half torque/capability of original system, the five-leg inverter can provide full torque/capability at up to half rated speed while has the same performance as the conventional fault tolerant control at rated speed. Fu and Lipo [21] proposed a method without changing the topology of dual three-phase machine drive; however, there method is only applicable for the system with only one neutral point, which is not suitable for the dual three-phase system with two isolated neutral points.

In this paper, the control of dual three-phase PMSM with two isolated neutral points based on five-leg inverter, the Topology 2 in Fig. 3(b), is investigated. Compared with the conventional dual three-phase inverter, the five-leg inverter can also fully fulfill the vector space decomposition (VSD) control [22] with reduced inverter leg at slow speed. Meanwhile, by dedicated selection of which two phases sharing the common leg, its current rating is approximately half of other phases' current rating. The five-leg inverter also has its disadvantages; the common problem of a five-leg inverter is that the dc bus voltage utilization is reduced to a half. Although the dc bus voltage utilization can increase a little bit from 0.5 to 0.5176, the improvement of dc bus voltage utilization is limited, which will be discussed at the end of the last paragraph in Section III. Meanwhile, due to the asymmetric inverter non-linearity, it will result in second harmonic current ripple. It can be mitigated by proper inverter non-linearity compensation, which will be validated in Section IV-B.

This paper is organized as follows. First, the principle of which two phases sharing the common leg is introduced in Section II-A. Second, the analysis of the five-leg inverter asymmetric non-linearity is detailed in Section II-B, which will result in the unbalanced currents. Then the current control of dual three-phase PMSM based on a five-leg inverter is proposed in Section III, and its steady-state operation without/with non-linearity compensation is evaluated and dynamical response performance is compared with the conventional dual three-phase inverter in Section IV.

II. Selection of Common Leg and Analysis of Inverter Non-Linearity

A. Selection of Common Leg

In the dual three-phase PMSM system, assuming the fundamental phase currents can be expressed as follows:

$$\begin{bmatrix} i_a \\ i_x \\ i_b \\ i_y \\ i_c \\ i_z \end{bmatrix} = I_m \cdot \begin{bmatrix} \cos(\theta + \pi/2 + \theta_x - 0 \cdot \theta_s) \\ \cos(\theta + \pi/2 + \theta_x - 1 \cdot \theta_s) \\ \cos(\theta + \pi/2 + \theta_x - 4 \cdot \theta_s) \\ \cos(\theta + \pi/2 + \theta_x - 5 \cdot \theta_s) \\ \cos(\theta + \pi/2 + \theta_x - 8 \cdot \theta_s) \\ \cos(\theta + \pi/2 + \theta_x - 9 \cdot \theta_s) \end{bmatrix} \tag{1}$$

where θ is the rotor electrical position, θ_x is the current lead angle for flux-weakening, I_m is the amplitude of phase currents, and $\theta_s = \pi/6$. If phase *C* in the first set of three-phase windings *ABC* is chosen to share the common leg with the other phase in the second set of three-phase windings *XYZ*, the sum current of phases *C* and *X*, phases *C* and *Y*, and phases *C* and *Z* with respect to $(\theta + \theta_x)$ is shown in Fig. 5. As can be seen from Fig. 5, to reduce the current rating of the common inverter leg, the phases

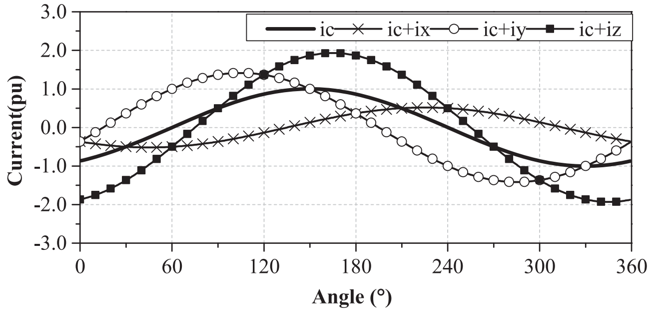

Fig. 5. Selection of phases as a pair to share the common leg.

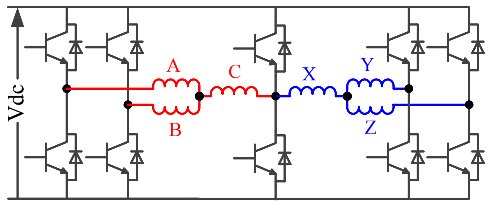

Fig. 6. Five-leg inverter for dual three-phase PMSM.

C and *X* should be chosen as a pair to share the common leg, whose current can be expressed as follows:

$$i_c + i_x = I_m \cos\left(\theta + \frac{\pi}{2} + \theta_x - 8\theta_s\right) + I_m \cos\left(\theta + \frac{\pi}{2} + \theta_x - \theta_s\right)$$
$$= 0.518 I_m \cos\left(\theta + \frac{\pi}{2} + \theta_x - \frac{9\theta_s}{2}\right). \quad (2)$$

As can be seen from (2), the current rating of common leg is only 0.518 times of the current rating of phases *C* or *X*. Therefore, the proposed power topology based on five-leg inverter for dual three-phase PMSM can be illustrated in Fig. 6.

Alternatively, phases *A* and *Y* or phases *B* and *Z* can also be chosen as a pair to share the common leg. In this paper, the scenario of phases *C* and *X* as a pair to share the common leg will be investigated.

B. Analysis of Inverter Non-Linearity

Take the five-leg inverter in Fig. 6 as an example, the phases *C* and *X* share the common leg; therefore, the general sinusoidal pulse width modulation (SPWM) or space vector pulse width modulation (SVPWM) cannot be employed directly. In this paper, a modified pulsewidth modulation (PWM) will be applied which will be introduced in Section III-B.

There are several causes to distort output voltage in the VSI [23]. Some are caused by the dead time that is inevitable to prevent the shoot-through phenomenon. Others originate from the inherent characteristics of the switching devices, such as the voltage drop, the output voltage transition slope, and the turn ON/OFF time. As detailed in [23] and [24], the distorted phase voltage resulted from inverter non-linearity is related to the phase current direction, which can be simplified as

$$V_{\text{phs\_dead}} = \text{sign}(i_{\text{phs}}) * V_{\text{dead}} \quad (3)$$

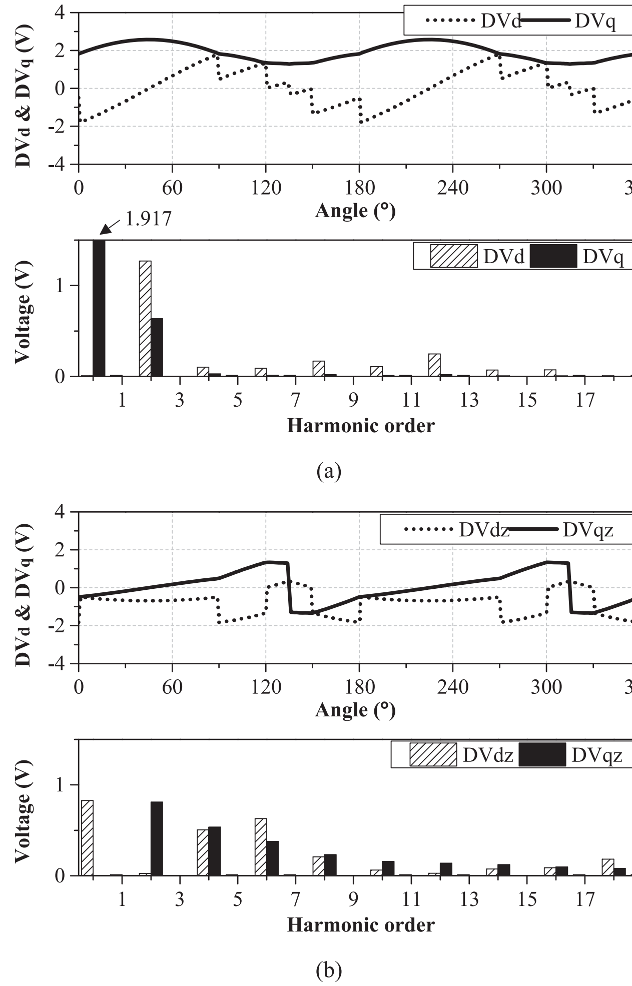

Fig. 7. Distorted voltage from inverter nonlinearity of five-leg inverter. (a) Distorted voltage in *dq*-frame. (b) Distorted voltage in *dqz*-frame.

where phs stands for phases *A*, *B*, *C*, *X*, *Y*, or *Z* in dual three-phase system. V_{dead} stands for the magnitude of distorted voltage.

In the five-leg inverter, the inverter non-linearity will result in unsatisfactory operation of drive system [25]. Since the phases *C* and *X* share common legs, the voltage distortion of phases *C* and *X* is the same, which is decided by the sign of common leg current. Therefore, the voltage distortion caused by five-leg inverter non-linearity can be expressed as

$$V_{\text{phs\_dead}} = \begin{cases} \text{sign}(i_{\text{phs}}) * V_{\text{dead}}, & \text{phs} = A, B, Y, Z \\ \text{sign}(i_c + i_x) * V_{\text{dead}}, & \text{phs} = C, X. \end{cases} \quad (4)$$

From (4), it can be concluded that the invert non-linearity for a single three-phase *ABC* or three-phase *XYZ* is asymmetrical.

Assuming V_{dead} is equal to 2 V, according to the VSD theory for dual three-phase system briefly introduced in the Appendix, applying the distorted phase voltage (4) to (A2) and then Park conversation and (A4), the distortion voltages in *dq*-frame in $\alpha\beta$ sub-plane and *dqz*-frame in z_1z_2 sub-plane can be obtained and illustrated in Fig. 7. DV_d and DV_q are the distorted *dq*-axis voltages in *dq*-frame. As can be seen, there is dominant dc voltage in DV_q and there are significant second harmonic voltages in DV_d and DV_q, which will result in second harmonic currents in

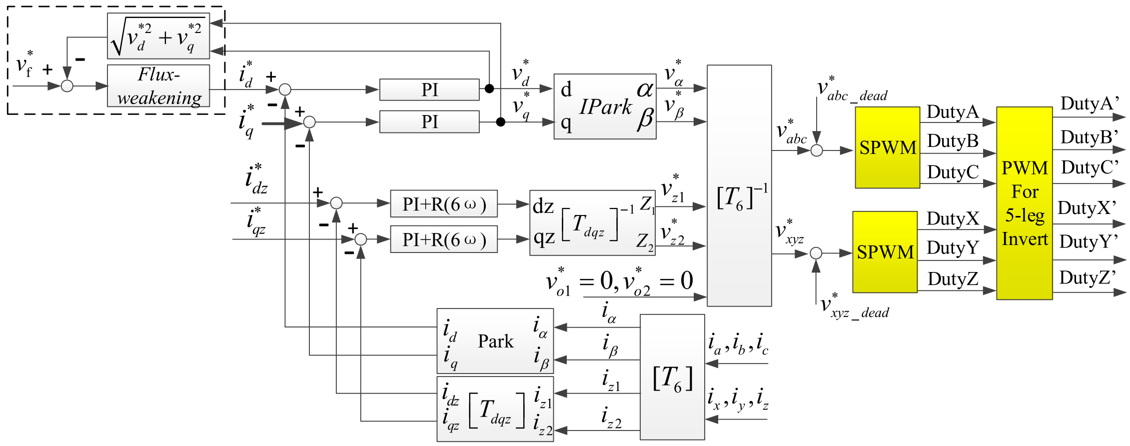

Fig. 8. VSD control of dual three-phase PMSM based on five-leg inverter.

dq-axis currents that means the currents between phases in each set are unbalanced [26]. DV_{dz} and DV_{qz} are the distorted voltages in *dqz*-frame in $z_1 z_2$ sub-plane; except the sixth harmonics, Fig. 7(b), which also exist in the conventional dual three-phase inverter and could be compensated by resonant control at the center frequency of sixth times of fundamental [26], [27], the dc, second, and other even order voltage distortions are also evident. The dc voltage distortion could be compensated by PI controller in *dqz*-frame. However, the second harmonic voltages will result in corresponding current harmonics in *dqz*-frame, which means the currents between two sets of three-phase windings are unbalanced [26].

In summary, the voltage distortion resulted from five-leg inverter non-linearity is more complicated than that caused by conventional dual three-phase drives [26]. The voltage distortion from five-leg inverter is asymmetric, which will result in current unbalance in the dual three-phase drive system if the inverter non-linearity is not compensated accurately.

III. Current Control Scheme

A. Current Control Scheme

The proposed current control is shown in Fig. 8, which is based on VSD theory for dual three-phase machine [22]. The fundamental and harmonics in i_a, i_b, i_c, i_x, i_y, and i_z in *abc-xyz*-frame are mapped as $\alpha\beta$, $z_1 z_2$, $o_1 o_2$ sub-planes, respectively, by matrix conversion in (A2), which are briefly introduced in the Appendix. Through Park conversion, the currents i_α, i_β in $\alpha\beta$ sub-plane are converted to currents in synchronous frame, i.e., *dq*-frame. Through matrix conversion of $[T_{dqz}]$ (see Appendix), the currents i_{z1}, i_{z2} in $z_1 z_2$ sub-plane are converted to currents in *dqz*-frame. Except the PI controllers in *dq*-frame and in *dqz*-frame, two resonant controllers [28]–[30] are employed to eliminate sixth harmonic currents in *dqz*-frame caused by inverter non-linearity [26], [27] and non-sinusoidal back EMF [26]. After the PWM duty for each phase is determined for conventional dual three-phase VSI, according to the principle of same line voltages, the PWM duty is modified to be applicable for five-leg inverters, which will be detailed in Section III-B.

To suppress the current unbalance resulted from five-leg inverter non-linearity, the distorted voltages are compensated by feed-forward compensation $v*_{\rm abc\_dead}$ and $v*_{\rm xyz\_dead}$ according to (4). The flux-weakening control is also illustrated in the dotted box in Fig. 8, where the amplitude of the fundamental voltage is employed as voltage feedback. If the fundamental voltage is higher than the voltage command v_f^*, the flux-weakening current i_d^* will decrease to a specific negative value to weaken the flux until the fundamental voltage is beyond the voltage reference v_f^*.

B. PWM Generation

For the three-phase system without the access of neutral point, the phase currents depend on the line voltages. Assuming the PWM duty for each phase is Duty*A*, Duty*B*, Duty*C*, Duty*X*, Duty*Y*, and Duty*Z*, respectively, in the conventional dual three-phase driver system. To maintain the same line voltages in five-leg inverter as that in conventional dual three-phase driver system, the PWM duty in the five-leg drive system can be calculated as follows.

Assuming the PWM duty for the common leg (phase *C* and *X*) is Duty_com, the modified PWM duty Duty*A'*, Duty*B'*, Duty*C'*, Duty*X'*, Duty*Y'*, and Duty*Z'* for phases *A*, *B*, *C*, *X*, *Y*, and *Z* in the five-leg drive, Fig. 6, can be expressed as

$$\text{Duty}A' = \text{Duty}A - \text{Duty}C + \text{Duty\_com} \tag{5}$$

$$\text{Duty}B' = \text{Duty}B - \text{Duty}C + \text{Duty\_com} \tag{6}$$

$$\text{Duty}C' = \text{Duty\_com} \tag{7}$$

$$\text{Duty}X' = \text{Duty\_com} \tag{8}$$

$$\text{Duty}Y' = \text{Duty}Y - \text{Duty}X + \text{Duty\_com} \tag{9}$$

$$\text{Duty}Z' = \text{Duty}Z - \text{Duty}X + \text{Duty\_com}. \tag{10}$$

The Duty_com of common leg is normally chosen as 0.5, as the duty of other phases are varied from 0 to 1; the line voltage can vary symmetrically from $-0.5*\text{Vdc}$ to $0.5*\text{Vdc}$, so the maximum line voltage in the region of linear modulation

TABLE I
PARAMETERS OF PROTOTYPE DUAL THREE-PHASE PMSM

Parameters	Value	Parameters	Value
Resistance (Ω)	1.096	Flux linkage (Wb)	0.075
Leakage inductance (mH)	0.875	Pole pairs	5
d-axis self-inductance (mH)	2.141	Power (W)	240
q-axis self-inductance (mH)	2.141	DC link voltage(V)	40

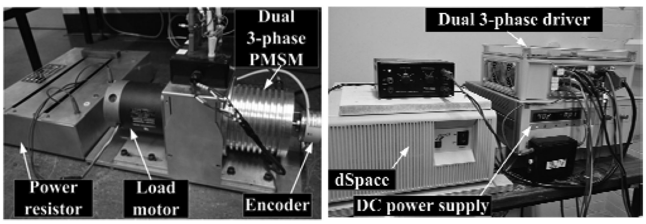

(a) (b)

Fig. 9. Experimental setup for dual three-phase PMSM drive. (a) Test rig of dual three-phase PMSM. (b) Dual three-phase drive system.

is 0.5∗Vdc, which is only half of the single three-phase drive system with SVPWM strategy [31], [32].

The dc bus voltage utilization is reduced to half, which is the common problem of five-leg inverter. It can be improved a little bit if the Duty_com could be adjusted timely while still maintaining the same line-to-line voltages [25], [33], which is similar to the SVPWM method in the single three-phase system with the zero sequence voltage injection [32], [33]. The dc bus voltage utilization can be improved from 0.5 to 0.5176 if the Duty_com is adjusted by 0.5∗(1- DutyMax – DutyMin), where

$$\text{DutyMax} = \max\begin{pmatrix}\text{Duty}A', \text{Duty}B', \text{Duty}C',\\ \text{Duty}X', \text{Duty}Y', \text{Duty}Z'\end{pmatrix} \tag{11}$$

$$\text{DutyMin} = \min\begin{pmatrix}\text{Duty}A', \text{Duty}B', \text{Duty}C',\\ \text{Duty}X', \text{Duty}Y', \text{Duty}Z'\end{pmatrix}. \tag{12}$$

The improvement of dc bus voltage utilization is not significant; therefore, the dual three-phase PMSM drive based on the five-leg inverter can be used in the scenario where there is enough dc bus voltage or in the scenario where full torque is required at low speed in the faulty condition.

IV. EXPERIMENTS

The hardware platform employed to investigate the control of the dual three-phase PMSM based on five-leg inverter is shown in Fig. 9. The test rig is based on dSPACE DS1005, two sets of three-phase insulated gate bipolar transistor (IGBT) intelligent power modules, STGIPS10K60A (600 V, 10 A) from STMicroelectronics, are utilized in the test rig. One phase of the second module of STGIPS10K60A is disabled deliberately to implement the five-leg inverter. The inverter power topology is the same as Fig. 6 with phases *C* and *X* as a pair to share the common leg. The execution rate of the current loop is the same as the PWM frequency of 10 kHz. The design parameters of the prototype dual three-phase PMSM are shown in Table I. The PMSM is coupled to a permanent magnet dc motor, which is connected to an adjustable power resistor used as load.

The purpose of the experiments is to demonstrate the VSD control of dual three-phase PMSM based on five-leg inverter without/with inverter non-linearity compensation. The overmodulation and flux-weakening control will not be considered and discussed in this paper. If there is enough dc bus voltage, the operation at high speed will not be an issue. In these experiments, the drive works in constant current mode with relatively slow speed, the i_q* is assigned as 1.5 A, i_d* is assigned to 0 A directly with flux-weakening control excluded. The design of PI gains is the same as that in [34], and the overall time delay including the PWM output delay, current sampling delay, and processing delay is approximately 1.5 times of PWM period. Thus, the optimized PI parameters can be derived by setting the damping factor to 0.707. The gains of resonant control for 6 ω are equal to the integral gain in the PI controller.

A. Comparison of Conventional and Five-Leg Inverter

In this experiment, the test results from conventional dual three-phase inverter and five-leg inverter are compared. Neither the inverter non-linearity of five-leg inverter nor the inverter non-linearity of conventional three-phase inverter is compensated; the drive works in constant current mode and the i_q reference is 1.5 A, the other current references, such as i_d, i_{dz}, and i_{qz} reference are zero.

When the conventional dual three-phase inverter is applied, the phase currents are shown in Fig. 10(a). The *dq*-axis currents i_d and i_q are shown in Fig. 10(b), and the currents in *dqz*-frame are shown in Fig. 10(c). From the harmonic analysis of *dq*-axis currents [see Fig. 10(d)] and *dqz*-axis currents [see Fig. 10(e)], it can be seen that the second harmonic currents are negligible.

When the five-leg inverter is employed for the dual three-phase PMSM, the phase currents are shown in Fig. 11(a). The currents of i_d and i_q are shown in Fig. 11 (b), and the currents of i_{dz} and i_{qz} are shown in Fig. 11(c). It is evident that there are second harmonic current ripples. Through the harmonic analysis of *dq*-axis currents [see Fig. 11(d)] and *dqz*-axis currents [see Fig. 11(e)], it can be seen that there are apparent second harmonic currents. As there are no second harmonic currents based on conventional dual three-phase inverter in Fig. 10(d) and (e), it indicates that the second harmonic currents in Fig. 11(d) and (e) are from the five-leg inverter, which is in accordance with the analysis in Section II-B.

The experimental results from conventional dual three-phase VSI set the benchmark for the five-leg inverter. By comparison, it can be concluded that the five-leg inverter can also fulfill the VSD control of the dual three-phase PMSM as well; meanwhile, the current of common leg is approximately half of the other legs' current, which is very beneficial for reduced inverter size and cost.

B. Unbalance Compensation for Five-Leg Inverter

If the voltage distortion resulted from the five-leg inverter non-linearity could be compensated effectively, the current unbalance can be mitigated. In this experiment, the voltage

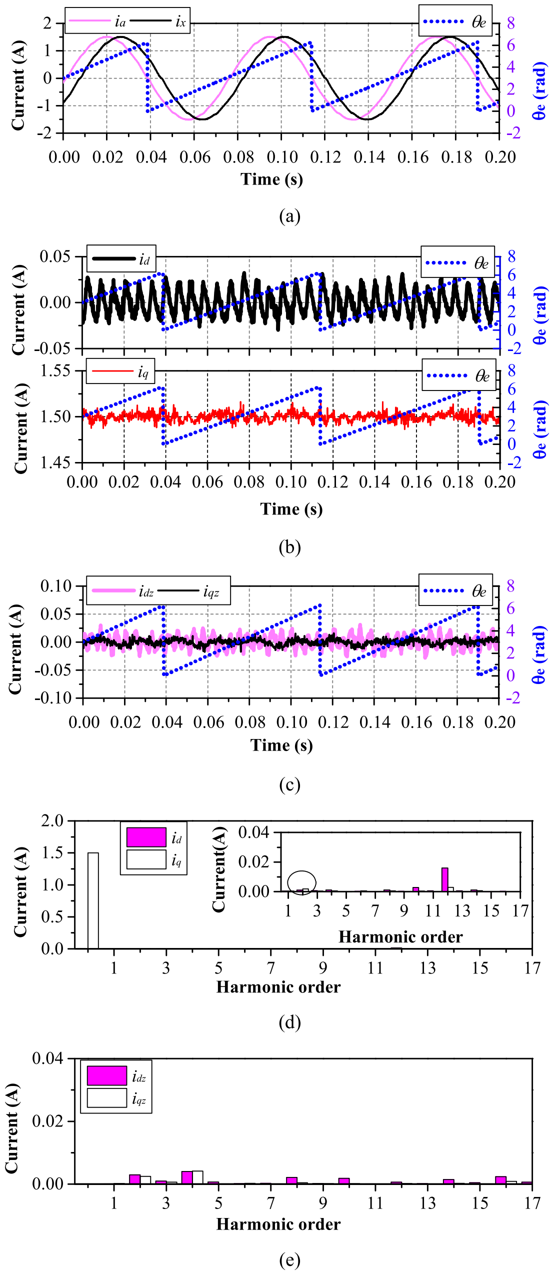

Fig. 10. VSD current control based on dual three-phase drive without inverter non-linearity compensation [PI in *dq*-frame and PI+R (sixth) in *dqz*-frame]. (a) Phase currents. (b) Currents in *dq*-frame. (c) Currents in *dqz*-frame. (d) Harmonics analysis of currents in *dq*-frame. (e) Harmonics analysis of currents in *dqz*-frame.

distortion is compensated according to the current direction (4) [23], [24]. The phases *A*, *B*, *Y*, and *Z* voltage distortion is compensated according to their current direction, respectively. Since the phases *C* and *X* share the common leg, their voltage distortions are compensated according to the direction of their total currents.

In this experiment, the drive also works in constant current mode and the i_q reference is 1.5 A. The experimental results of five-leg inverter are shown in Fig. 12. Compared with the experimental results of five-leg inverter without inverter

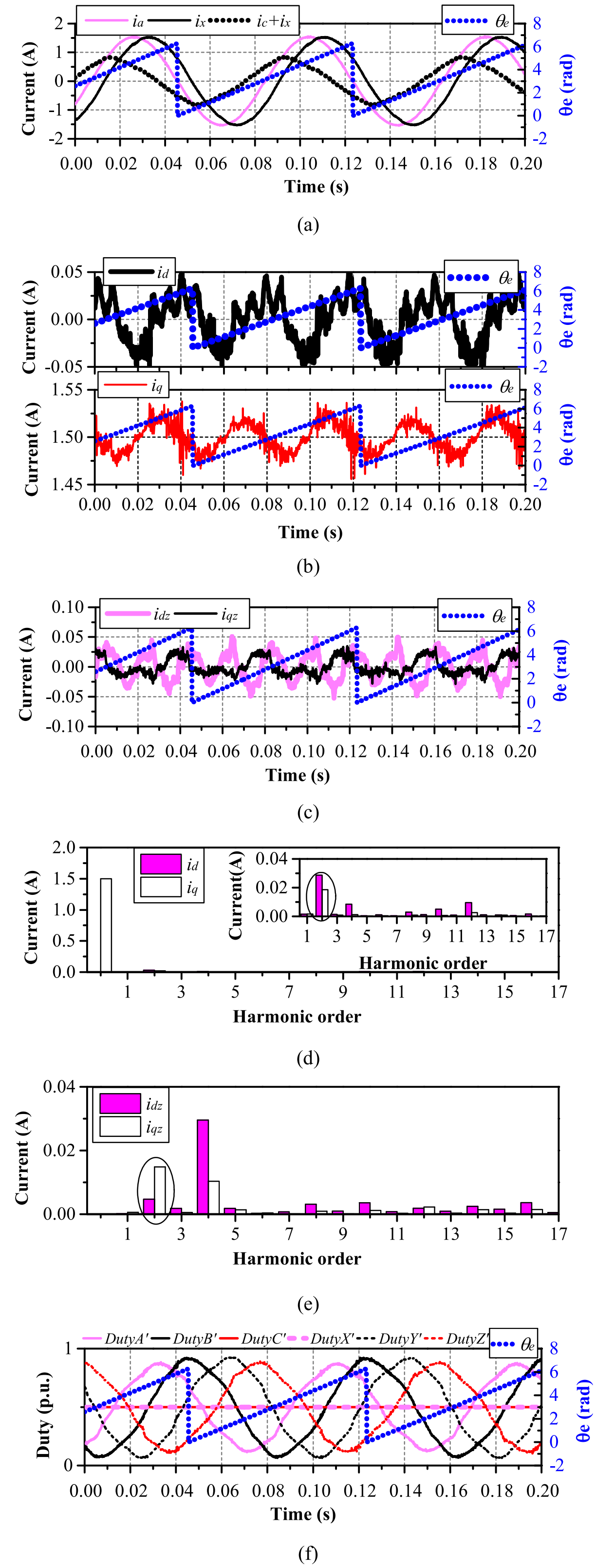

Fig. 11. VSD current control-based five-leg inverter without inverter non-linearity compensation (PI in *dq*-frame and PI+R (sixth) in *dqz*-frame). (a) Phase currents. (b) Currents in *dq*-frame. (c) Currents in *dqz*-frame. (d) Harmonics analysis of currents in *dq*-frame. (e) Harmonics analysis of currents in *dqz*-frame. (f) PWM duty.

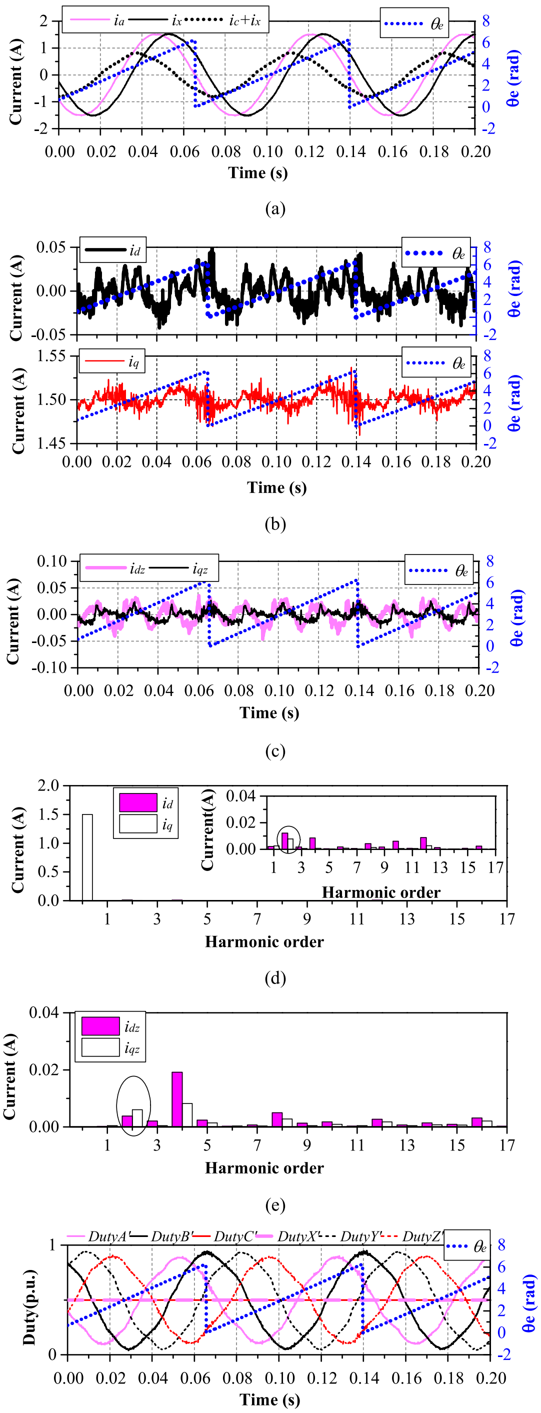

Fig. 12. VSD current control-based five-leg inverter with inverter nonlinearity compensation (PI in *dq*-frame and PI+R(sixth) in *dqz*-frame) (a) Phase currents. (b) Currents in *dq*-frame. (c) Currents in *dqz*-frame. (d) Harmonics analysis of currents in *dq*-frame. (e) Harmonics analysis of currents in *dqz*-frame. (f) PWM duty.

nonlinearity compensation (see Fig. 11), it can be found that the *dq*-axis currents [see Fig. 12(b)] have much smaller current ripples than that in Fig. 11(b). The *dq*-axis current harmonic analysis [see Fig. 12(d)] and *dqz*-axis current harmonic analysis [see Fig. 12(e)] show that there are less second harmonics than

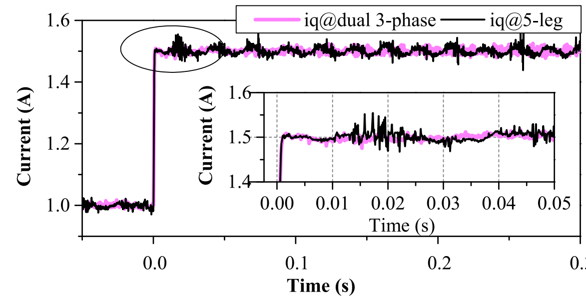

Fig. 13. Step response.

that in Fig. 11(d) and (e), respectively. However, due to inaccurate feed-forward voltage compensation, there are still a small portion of second harmonic currents.

C. Dynamic Performance

In the evaluation of dynamic performance, the i_q reference is stepped from 1.0 to 1.5 A at the time stamp of zero second. The current step response from dual three-phase inverter and five-leg inverter is compared. The experimental results are shown in Fig. 13, it can be seen that the dual three-phase VSD control based on dual three-phase inverter and five-leg inverter have equivalent rising time and settling time, which means the five-leg inverter has the equivalent dynamical response to the dual three-phase inverter.

V. Conclusion

The current control of dual three-phase PMSM base on five-leg inverter is investigated in this paper. It can fully fulfill the VSD control of dual three-phase PMSM and has the equivalent dynamical response to the dual three-phase inverter. With dedicated selection of phase from each set of single three-phase windings as a pair to share the common leg, the current rating of the common leg is approximately half of the rating of other legs. Meanwhile, the five-leg inverter non-linearity is analyzed in detail. With the inverter non-linearity feed-forward compensation, the current unbalance could be mitigated in steady-state operation without deterioration of dynamical performance.

Appendix

According to VSD theory [22], the original six-dimensional machine system can be decomposed into three orthogonal subspaces, i.e., $\alpha\beta$, z_1z_2, o_1o_2 sub-planes. By using the transformation matrix, which is shown in (A1), different harmonics are projected to different sub-planes

$$[T_6] = \frac{1}{3}\begin{bmatrix} 1 & \cos(\theta_s) & \cos(4\theta_s) & \cos(5\theta_s) & \cos(8\theta_s) & \cos(9\theta_s) \\ 0 & \sin(\theta_s) & \sin(4\theta_s) & \sin(5\theta_s) & \sin(8\theta_s) & \sin(9\theta_s) \\ 1 & \cos(5\theta_s) & \cos(8\theta_s) & \cos(\theta_s) & \cos(4\theta_s) & \cos(9\theta_s) \\ 0 & \sin(5\theta_s) & \sin(8\theta_s) & \sin(\theta_s) & \sin(4\theta_s) & \sin(9\theta_s) \\ 1 & 0 & 1 & 0 & 1 & 0 \\ 0 & 1 & 0 & 1 & 0 & 1 \end{bmatrix} \tag{A1}$$

where $\theta_s = \pi/6$. The fundamental and (12k ± 1)th, k ∈ (1, 2, 3, . . .) harmonics in *abc*-frame are mapped to $\alpha\beta$ sub-plane; the (6k ± 1)th, k ∈ (1, 3, 5, . . .) harmonics in *abc*-frame are mapped to z_1z_2 sub-plane; and the (3k)th, k ∈ (1, 3, 5, . . .) harmonics in *abc*-frame are mapped to o_1o_2 sub-plane. The transformation can be described as follows:

$$\begin{aligned} &\left[F_\alpha \ F_\beta \ F_{z1} \ F_{z2} \ F_{o1} \ F_{o2} \right]^T \\ &\quad = [T_6] \cdot \left[F_a \ F_x \ F_b \ F_y \ F_c \ F_z \right]^T \end{aligned} \tag{A2}$$

where F is v, i, or ψ, which are corresponding to voltage, current, and stator flux, respectively.

If we define $[T_{dqz}]$ as (A3) and a new matrix conversion as (A4) [26], by this matrix conversion, the variables in z_1z_2 sub-plane are converted to a new frame, which can be designated as *dqz*-frame. Consequently, all the (6k ± 1)th, k ∈ (1, 3, 5, . . .) harmonics in z_1z_2 sub-plane are converted to (6k)th harmonics in *dqz*-frame

$$[T_{dqz}] = \begin{bmatrix} -\cos\theta & \sin\theta \\ \sin\theta & \cos\theta \end{bmatrix} \tag{A3}$$

$$\begin{bmatrix} F_{dz} \\ F_{qz} \end{bmatrix} = [T_{dqz}] \begin{bmatrix} F_{z1} \\ F_{z2} \end{bmatrix}. \tag{A4}$$

Reference

[1] T. M. Jahns, "Improved reliability in solid-state AC drives by means of multiple independent phase drive units," *IEEE Trans. Ind. Appl.*, vol. IA-16, no. 3, pp. 321–331, May 1980.

[2] G. K. Singh, K. Nam, and S. K. Lim, "A simple indirect field-oriented control scheme for multiphase induction machine," *IEEE Trans. Ind. Electron.*, vol. 52, no. 4, pp. 1177–1184, Aug. 2005.

[3] E. Levi, R. Bojoi, F. Profumo, H. A. Toliyat, and S. Williamson, "Multiphase induction motor drives - A technology status review," *IET Elect. Power Appl.*, vol. 1, no. 4, pp. 489–516, Jul. 2007.

[4] E. Levi, "Multiphase electric machines for variable-speed applications," *IEEE Trans. Ind. Electron.*, vol. 55, no. 5, pp. 1893–1909, May 2008.

[5] F. Barrero and M. J. Duran, "Recent advances in the design, modeling, and control of multiphase machines—Part I," *IEEE Trans. Ind. Electron.*, vol. 63, no. 1, pp. 449–458, Jan. 2016.

[6] S. Hu, Z. Liang, W. Zhang, and X. He, "Research on the integration of hybrid energy storage system and dual three-phase PMSM drive in EV," *IEEE Trans. Ind. Electron.*, vol. 65, no. 8, pp. 6602–6611, Aug. 2018.

[7] K. Gopakumar, S. Sathiakumar, S. K. Biswas, and J. Vithayathil, "Modified current source inverter fed induction motor drive with reduced torque pulsations," *Inst. Elect. Eng. Proc. B-Elect. Power Appl.*, vol. 131, no. 4, pp. 159–164, 1984.

[8] K. Gopakumar, V. T. Ranganthan, and S. R. Bhat, "Split-phase induction motor operation from PWM voltage source inverter," *IEEE Trans. Ind. Appl.*, vol. 29, no. 5, pp. 927–932, Sep./Oct. 1993.

[9] H. W. Van der Broeck and J. D. Van Wyk, "A comparative investigation of a three-phase induction machine drive with a component minimized voltage-fed inverter under different control options," *IEEE Trans. Ind. Appl.*, vol. IA-20, no. 2, pp. 309–320, Mar. 1984.

[10] Z. Zeng, W. Zheng, R. Zhao, C. Zhu, and Q. Yuan, "Modeling, modulation, and control of the three-phase four-switch PWM rectifier under balanced voltage," *IEEE Trans. Power Electron.*, vol. 31, no. 7, pp. 4892–4905, Jul. 2016.

[11] K. Gi-Taek and T. A. Lipo, "VSI-PWM rectifier/inverter system with a reduced switch count," *IEEE Trans. Ind. Appl.*, vol. 32, no. 6, pp. 1331–1337, Nov./Dec. 1996.

[12] E. Ledezma, B. McGrath, A. Munoz, and T. A. Lipo, "Dual AC-drive system with a reduced switch count," *IEEE Trans. Ind. Appl.*, vol. 37, no. 5, pp. 1325–1333, Sep./Oct. 2001.

[13] T. Lixin and S. Gui-Jia, "High-performance control of two three-phase permanent-magnet synchronous machines in an integrated drive for automotive applications," *IEEE Trans. Power Electron.*, vol. 23, no. 6, pp. 3047–3055, Nov. 2008.

[14] P. Delarue, A. Bouscayrol, and B. Francois, "Control implementation of a five-leg voltage-source-inverter supplying two three-phase induction machines," in *Proc. IEEE Int. Elect. Mach. Drives Conf.*, 2003, vol. 3, pp. 1909–1915.

[15] T. Lixin, S. Gui-Jia, and H. Xianghui, "Experimental high-performance control of two permanent magnet synchronous machines in an integrated drive for automotive applications," *IEEE Trans. Power Electron.*, vol. 23, no. 2, pp. 977–984, Mar. 2008.

[16] Y. Kimura, M. Hizume, and K. Matsuse, "Independent vector control of two PM motors with five-leg inverter by the expanded two-arm modulation method," in *Proc. Eur. Conf. Power Electron. Appl.*, 2005, pp. 1–7.

[17] K. Oka and K. Matsuse, "PWM technique of five-leg inverter applying two-arm modulation," *IEEJ Trans. Ind. Appl.*, vol. 129, pp. 811–816, 2009.

[18] D. Zhou, J. Zhao, and Y. Li, "Model-predictive control scheme of five-leg AC-DC-AC converter-fed induction motor drive," *IEEE Trans. Ind. Electron.*, vol. 63, no. 7, pp. 4517–4526, Jul. 2016.

[19] W. Wang, J. Zhang, and M. Cheng, "A dual-level hysteresis current control for one five-leg VSI to control two PMSMs," *IEEE Trans. Power Electron.*, vol. 32, no. 1, pp. 804–814, Jan. 2017.

[20] B. Tabbache, M. Benbouzid, K. Marouani, and A. Kheloui, "A decoupled control of 5-legs PWM inverter feeding a two induction motors-based electric vehicle powertrain," *J. Elect. Syst.*, vol. 12, pp. 460–474, 2016.

[21] J. R. Fu and T. A. Lipo, "Disturbance-free operation of a multiphase current-regulated motor drive with an opened phase," *IEEE Trans. Ind. Appl.*, vol. 30, no. 5, pp. 1267–1274, Sep./Oct. 1994.

[22] Y. Zhao and T. A. Lipo, "Space vector PWM control of dual three-phase induction machine using vector space decomposition," *IEEE Trans. Ind. Appl.*, vol. 31, no. 5, pp. 1100–1109, Sep./Oct. 1995.

[23] J. W. Choi and S. K. Sul, "Inverter output voltage synthesis using novel dead time compensation," *IEEE Trans. Power Electron.*, vol. 11, no. 2, pp. 221–227, Mar. 1996.

[24] H. S. Kim, K. H. Kim, and M.-J. Youn, "On-line dead-time compensation method based on time delay control," *IEEE Trans. Control Syst. Technol.*, vol. 11, no. 2, pp. 279–285, Mar. 2003.

[25] D. Dujic, M. Jones, S. N. Vukosavic, and E. Levi, "A general PWM method for a ($2n+$ 1)-leg inverter supplying n three-phase machines," *IEEE Trans. Ind. Electron.*, vol. 56, no. 10, pp. 4107–4118, Oct. 2009.

[26] Y. Hu, Z. Q. Zhu, and K. Liu, "Current control for dual three-phase PM synchronous motors accounting for current unbalance and harmonics," *IEEE J. Emerg. Sel. Topics Power Electron.*, vol. 2, no. 2, pp. 272–284, Jun. 2014.

[27] H. S. Che, E. Levi, M. Jones, W. P. Hew, and N. A. Rahim, "Current control methods for an asymmetrical six-phase induction motor drive," *IEEE Trans. Power Electron.*, vol. 29, no. 1, pp. 407–417, Jan. 2014.

[28] D. N. Zmood, D. G. Holmes, and G. H. Bode, "Frequency-domain analysis of three-phase linear current regulators," *IEEE Trans. Ind. Appl.*, vol. 37, no. 2, pp. 601–610, Mar./Apr. 2001.

[29] D. N. Zmood and D. G. Holmes, "Stationary frame current regulation of PWM inverters with zero steady-state error," *IEEE Trans. Power Electron.*, vol. 18, no. 3, pp. 814–822, May 2003.

[30] L. R. Limongi, R. Bojoi, G. Griva, and A. Tenconi, "Digital current-control schemes," *IEEE Ind. Electron. Mag.*, vol. 3, no. 1, pp. 20–31, Mar. 2009.

[31] J. A. Houldsworth and D. A. Grant, "The use of harmonic distortion to increase the output voltage of a three-phase PWM inverter," *IEEE Trans. Ind. Appl.*, vol. IA-20, no. 5, pp. 1224–1228, Sep. 1984.

[32] C. Dae-Woong, K. Joohn-Sheok, and S. Seung-Ki, "Unified voltage modulation technique for real-time three-phase power conversion," *IEEE Trans. Ind. Appl.*, vol. 34, no. 2, pp. 374–380, Mar./Apr. 1998.

[33] Z. Keliang and W. Danwei, "Relationship between space-vector modulation and three-phase carrier-based PWM: A comprehensive analysis [three-phase inverters]," *IEEE Trans. Ind. Electron.*, vol. 49, no. 1, pp. 186–196, Feb. 2002.

[34] V. Blasko, V. Kaura, and W. Niewiadomski, "Sampling of discontinuous voltage and current signals in electrical drives: A system approach," *IEEE Trans. Ind. Appl.*, vol. 34, no. 5, pp. 1123–1130, Sep./Oct. 1998.

Yashan Hu received the B.Eng. and M.Sc. degrees from Northwestern Polytechnical University, Xi'an, China, in 2002 and 2005, respectively, and the Ph.D. degree from the University of Sheffield, Sheffield, U.K., in 2016, all in electronic and electrical engineering.

From 2016 to 2018, he was an Advanced Research Engineer with Siemens Wind Power A/S, Denmark. Since 2018, he has been an Associate Professor with the College of Electrical and Information Engineering, Hunan University, Changsha, China. His current research interests include power electronic systems and control and wind energy conversion systems.

Shoudao Huang (SM'14) was born in Hunan, China, in 1962. He received the B.S. and Ph.D. degrees in electrical engineering from the College of Electrical and Information Engineering, Hunan University, Changsha, China, in 1983 and 2005, respectively.

He is currently a Full Professor with the College of Electrical and Information Engineering, Hunan University. His research interests include motor design and control, power electronic systems and control, and wind energy conversion systems.

Xuan Wu received the Ph.D. degree in automation from Hunan University, Changsha, China, in 2016.

He is currently a Postdoctoral Fellow with the College of Electrical and Information Engineering, Hunan University. His research interests include permanent magnet synchronous motor drives and position sensorless control of ac motors.

Xuefei Li received the B.Eng. degree in electronic and electrical engineering from the Northwestern Polytechnical University, Xi'an, China, in 2003.

Since 2018, she has been a Research Assistant with the College of Electrical and Information Engineering, Hunan University, Changsha, China. Her current research interests include power electronic systems and control and renewable energy.